CONFERENCE & EXHIBITION
NEAR SURFACE GEOSCIENCE'19

EAGE

Seismic reflection imaging of fractures using least-squares migration and linear-slip theory: laboratory and numerical tests

Shohei Minato, Delft University of Technology and OYO Corporation,
Ranajit Ghose, and Kees Wapenaar, Delft University of Technology

Summary

Characterizing the mechanical and hydraulic properties of fractures is crucial in hydrocarbon and geothermal field development. Contrary to passive microseismic measurements, active seismic measurements using a borehole, e.g., VSP or sonic logging, have a potential to address aseismic fractures. However, there is a considerable scale gap between the characteristic wavelength in VSP and in sonic logging, which hinders consistent interpretations of active and passive measurements. Recent developments of reflection imaging using microearthquakes and dipole acoustic data successfully image individual fractures or clusters of them around a borehole, which indicates the potential to fill the gap by addressing quantitative fracture properties around a borehole up to a few tens of meters away from the borehole. In this study, we couple the least-squares migration with the linear-slip theory in order to achieve high-resolution reflection imaging of fracture compliances around a borehole, which are then useful to characterize microscale structures at the fracture. Tests in the laboratory successfully characterize the spatially varying fracture compliance due to the partial inclusion of water in the fracture. Numerical modelling tests of the source-receiver configuration of acoustic dipole measurements and random background media shows the potential of the proposed approach for quantitatively imaging fractures around a borehole.

Introduction

Characterization of the mechanical and hydraulic properties of fractures is crucial in hydrocarbon exploration and geothermal field development. Active seismic methods have been developed to complement the passive microseismic measurements (Niitsuma et al., 1999), and they have been successfully applied to geothermal field; VSP/crosshole seismic measurements have located fractured zone (e.g., Green et al., 1989) and sonic logging is commonly performed to obtain sonic velocity around a borehole. Fracture characterization using seismic anisotropy, e.g., shear-wave splitting in VSP and dipole acoustic data, has been successfully applied in hydrocarbon exploration (Prioul and Jocker, 2009) where the effective medium approach is key to connecting the multi-scale borehole data, i.e., borehole televiewer (BHTV), formation microimager (FMI), dipole sonic imager (DSI), and VSP.

However, structures and physical properties obtained from the active seismic measurements (e.g., reflection/attenuation structures from VSP and sonic velocities) are not directly associated to those obtained from passive microseismic measurements (e.g., location and orientation of active fractures and possible fluid pathways in a reservoir). This is mainly because passive methods are sensitive to seismic fractures and there is a large gap between the available wavelengths in active methods: VSP with wavelength of a few hundred meters and sonic logging sensing a few decimetres around a borehole. The active seismic data and processing techniques between these two distinct scales are crucial for deciphering a link between the interpretations from the active and passive measurements. In this vein, the earlier study of high-frequency reflection imaging using microearthquakes (wavelength of a few tens of meters) predicted the presence of fractures (e.g., Reshetnikov et al., 2010), and the recent developments in shear-wave reflection imaging using acoustic dipole tools enable using the wavelength of 1–2 meters to reveal structures around a borehole (Tang and Patterson, 2009). More recently, Lee et al. (2019) used cross-dipole data and successfully imaged fine structures at a fault system in crystalline rocks around a borehole up to 30 m away from the borehole.

In such intermediate-scale measurements, we consider that fractures are elastic heterogeneities producing scattered waves. The linear slip theory (Schoenberg, 1980) is useful to represent the heterogeneity where fractures are considered zero-thickness compliant interfaces. The seismic wave is characterized by the fracture compliance tensor which is a function of micro-scale structures at a fracture, i.e., aperture, infill materials and statistical properties of asperity distribution (e.g., Worthington and Hudson, 2000). In the hydraulic fracture experiments, the dilation at a fracture due to shearing and corresponding transient increase of the hydraulic permeability are controlled by the fracture roughness (Nemoto et al., 2008). In this regard, the fracture compliance tensor is sensitive to the change of coupling/asperity distribution at a rough fracture due to shearing (Nakagawa et al., 2000). The fracture compliances are also useful in predicting the existence of fluid in a fracture (Lubbe et al., 2008). Therefore, characterizing fractures using linear-slip theory should provide useful information for hydrocarbon/geothermal field developments.

In this study, we propose to characterize linear-slip interfaces (fractures) using reflected waves due to a single fracture or clusters of fractures observed in a borehole, e.g., acoustic logging. In order to achieve high-resolution quantitative imaging, we consider the least-squares migration which offers high-resolution results for sparse, irregularly sampled data (Nemeth et al., 1999). We couple the least-squares migration with the linear-slip theory; we solve linearized waveform inversion to estimate spatial distribution of fracture compliances. We explore this concept using laboratory and numerical experiments considering borehole measurements.

Theory

We consider the linear-slip theory with a rotationally invariant fracture (Schoenberg, 1980); $\Delta\mathbf{u}=\mathrm{diag}(\eta_T, \eta_T, \eta_N)\,\boldsymbol{\tau}$, where $\Delta\mathbf{u}$ is the seismic displacement-discontinuity vector and $\boldsymbol{\tau}$ traction vector at the fracture. η_T and η_N are, respectively, tangential and normal fracture compliance.

The least-squares migration solves the following linearized waveform inversion:

$$\mathbf{d} = \mathbf{Lm} \quad (1)$$

where **d** denotes the seismic data (frequency domain in this study), **L** the Born or Kirchhoff operator, and **m** the model parameters at each spatial grid point. In this study, **m** is the fracture compliances (η_T and η_N), and **L** is the Born operator including Green's function, source wavelet, and fracture dip. We derive the linearized equation using the general formulation for the boundary integral representation of seismic wavefield including linear-slip interfaces (Wapenaar, 2007). More explicit form of equation (1) can be found in Minato et al. (2018b) where the accuracy of the Born approximation (equation (1)) was discussed. In this study, we solve equation (1) using conjugate gradient method for laboratory experimental data and truncated SVD for numerical modelling data with full matrix **L**.

Laboratory experiments

We apply the theory to laboratory experimental data where we measure PP reflection responses from an artificial vertical fracture (Figure 1(a)). The background material is aluminum, the fracture does not have contact asperities, and the fracture aperture is controlled to be approximately 100 μm. We use piezo-electric transducers for transmitter and receiver, producing and recording displacements in *x* direction. The PP reflected waves from the fracture was observed with the centre frequency of 700 kHz. The data was originally designed for AVO analyses (Minato 2018a), and we interpret the measurement geometry to borehole experiments for vertical fractures where sources and receivers are located on the same lateral (*x*) position. Contrary to our previous presentation (Minato et al., 2018b), in this study, we further estimate source functions and provide quantitative imaging results.

The PP reflection response was measured considering three different fracture conditions; dry fracture (i.e., air is filled in the fracture), homogeneously wet fracture (i.e., water is filled in the fracture), and heterogeneously wet fracture (i.e., a part of the fracture is filled with water and the other with air, see Figure 1(a)). We collected 21 shot gathers and each shot gather contained on average 20 receivers. More detailed measurement procedure can be found in Minato et al. (2018a). We first estimate source functions from the dry fracture response; we deconvolve recorded dry response with the theoretical dry response calculated by free-surface reflection coefficients and Kirchhoff approximation.

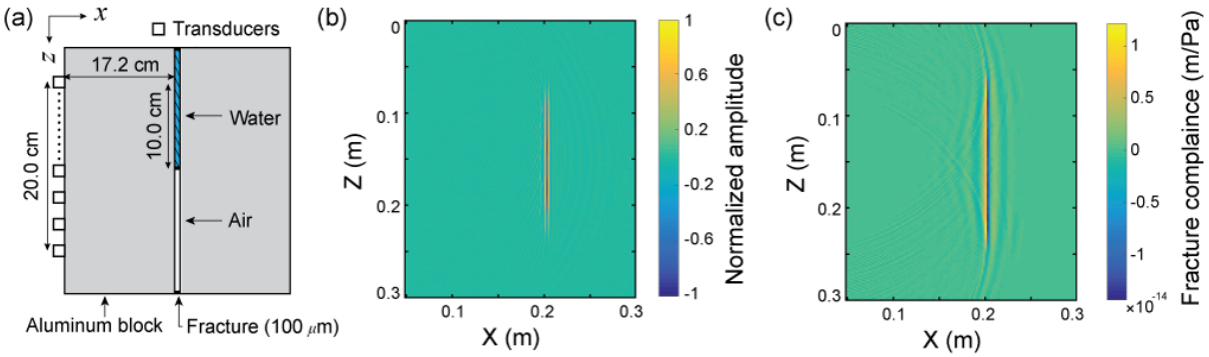

Figure 1 *(a) Configurations of laboratory experiments. (b) Imaging result with conventional reverse-time migration. (c) Imaging result with the proposed least-squares migration.*

Figure 1(c) shows the result of the least-squares migration for the homogeneous wet fracture. We estimate the distribution of normal compliance assuming the values of tangential compliance to be very large, representing no contact asperities. We also show the result of conventional reverse-time migration (Figure 1(b)). It is clear that the sharp, better-illuminated image is obtained due to the least-squares migration (Figure 1(c)). The values of imaged normal compliance are 0.9–1.3×10^{-14} m/Pa, which are smaller than the results of AVO analyses (6–9×10^{-14} m/Pa, Minato et al., 2018a). Underestimation of fracture compliance was expected (Minato et al., 2018b) because the Born approximation overpredicts amplitudes. Figure 2 shows the imaged compliance values along the fracture geometry for the different fracture conditions. It is clear that the homogeneously wet fracture

(black line) is uniformly stiffer than the dry fracture (blue line). On the other hand, the heterogeneous fracture (red line) shows the clear transition of the compliance from wet to dry condition. In conclusion, we can successfully estimate fracture compliances with high resolution by least-squares migration, and detect the changes in the normal compliance due to the inclusion of water in the fracture.

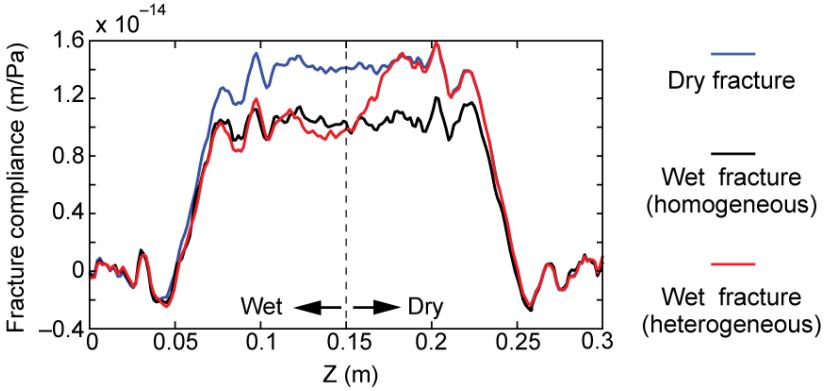

Figure 2 *Estimated normal fracture compliances at three different fracture conditions.*

Numerical example of fracture imaging using dipole acoustic data

We perform numerical modelling considering the geometry of borehole sonic logging in order to image a single dipping fracture that has a few tens of meter length embedded in a random background medium (Figure 3(a)). We consider 2D problem where dipole acoustic measurements are separately modelled by P-SV and SH wavefields using FDTD method. A fluid-filled fracture with rough surface is assumed ($\eta_T = 1\times10^{-11}$, $\eta_N = 1\times10^{-12}$), where fracture compliances and their magnitudes are taken from literature (Lubbe et al., 2008; Hobday and Worthington, 2012). We consider realistic source and receiver configuration for dipole acoustic measurements; receiver array consists of 5 receivers with minimum offset 0.3 m and receiver spacing 0.15 m, and the tool moves along the borehole in steps of 0.5m (e.g., Li et al., 2017). We use Ricker wavelet of 2 kHz centre frequency for source wavelet to simulate the realistic dominant frequency. Note that for simplicity we ignore the effect of a fluid-filled borehole. Contrary to the work discussed in the previous section, we now estimate tangential compliance using the least-squares migration; we evaluate the dominant effect of tangential compliance of fluid-filled rough fracture and the sensitivity of dipole data to shear-wave velocity structures. Furthermore, we assume that the data has been carefully filtered (e.g., Li et al., 2017) so that it contains only scattered (reflected) waves. Green's function of homogeneous medium is assumed in the imaging (**L** in equation (1)).

The results of the least-squares migration (Figures 4(b) and 4(c)) clearly show that the high-resolution quantitative fracture imaging is possible in the source-receiver geometry of dipole acoustic measurements and for a random background medium. An X-shaped artefact in Figure 4(b) shows ambiguity in the fracture location, but it could be suppressed by wavefield separation prior to imaging (e.g., Tang and Patterson, 2009).

Conclusion

We have developed a least-squares migration for imaging fracture compliances with high resolution. Using the laboratory experimental data, we have successfully characterized the spatially varying fracture where water is included partially in the fracture. Numerical modelling of realistic source and receiver geometry of acoustic dipole measurements with random background media shows the potential of the proposed approach for quantitatively imaging fractures around a borehole. The methodology will be crucial in filling the scale gap between the acoustic logging and controlled-source seismic measurements (e.g., VSP) and in providing in-situ mechanical and hydraulic fracture properties.

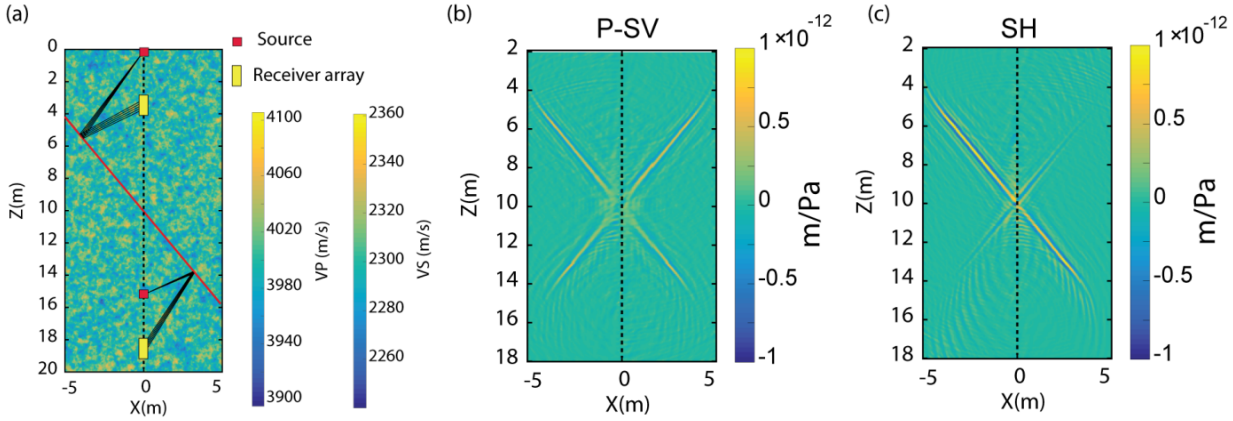

Figure 4 *(a) Configuration of the numerical modelling. (b) Imaging result of the least-squares migration for P-SV wavefield. (c) Same as (b) but for SH wavefield.*

References

Green, A. S. P., Baria, R. and Jones, R. [1989] VSP and Cross-hole seismic surveys used to determine reservoir characteristics of a hot dry rock geothermal system. *International Journal of Rock Mechanics and Mining Sciences & Geomechanics Abstracts*, **26**(3), 271–280.

Nemeth, T., C. Wu, and G. T. Schuster [1999] Least-squares migration of incomplete reflection data. *Geophysics*, **64**, 208–221.

Hobday, C., and Worthington, M. [2012] Field measurements of normal and shear fracture compliance. *Geophysical Prospecting*, **60**, 488–499.

Lee, S. Q., Tang, X. M. and Su, Y. D. [2019] Shear wave imaging to determine near-borehole faults for ocean drilling exploration. *Geophysical Journal International*, **217**, 288–293.

Li, J., Innanen, K. A. and Tao, G. [2017] Extraction of reflected events from sonic-log waveforms using the Karhunen-Loève transform. *Geophysics*, **82**(5), D265–D277.

Lubbe, R., Sothcott, J., Worthington, M. and McCann, C. [2008] Laboratory estimates of normal and shear fracture compliance. *Geophysical Prospecting*, **56**, 239–247.

Minato, S., Ghose, R. and Osukuku, G. [2018a] Experimental verification of spatially varying fracture-compliance estimates obtained from amplitude variation with offset in version coupled with linear slip theory. *Geophysics*, **83**, WA1–WA8.

Minato, S., Ghose, R. and Wapenaar, K. [2018b] Seismic modelling and inversion of nonwelded interfaces using the boundary integral equation. *Proceedings of the 13th SEGJ International Symposium*.

Nakagawa, S., Nihei, K. and Myer, L. [2000] Shear-induced conversion of seismic waves across single fractures. *International Journal of Rock Mechanics and Mining Sciences*, **37**, 203–218.

Nemoto, K., Moriya, H., Niitsuma, H. and Tsuchiya, N. [2008] Mechanical and hydraulic coupling of injection-induced slip along pre-existing fractures. *Geothermics*, **37**(2), 157–172.

Niitsuma, H., Fehler, M., Jones, R., Wilson, S., Albright, J., Green, A., Baria, R., Hayashi, K., Kaieda, H., Tezuka, K., Jupe, A., Wallroth, T., Cornet, F., Asanuma, H., Moriya, H., Nagano, K., Phillips, W. S., Rutledge, J., House, L., Beauce, A., Alde, D. and Aster, R. [1999] Current status of seismic and borehole measurements for HDR/HWR development. *Geothermics*, **28**(4), 475–490.

Prioul, R. and Jocker, J. [2009] Fracture characterization at multiple scales using borehole images, sonic logs, and walkaround vertical seismic profile. *AAPG bulletin*, **93**(11), 1503–1516.

Reshetnikov, A., Buske, S. and Shapiro, S. A. [2010] Seismic imaging using microseismic events: Results from the San Andreas Fault System at SAFOD, *Journal of Geophysical Research: Solid Earth*, **115** (B12324).

Schoenberg, M. [1980] Elastic wave behavior across linear slip interfaces. *The Journal of the Acoustical Society of America*, **68**, 1516–1521.

Tang, X. M., and Patterson, D. J. [2009] Single-well S-wave imaging using multicomponent dipole acoustic-log data. *Geophysics*, **74**, WCA211–WCA223.

Wapenaar, K. [2007] General representations for wavefield modeling and inversion in geophysics. *Geophysics*, **72**, SM5–SM17.

Worthington, M. H., and Hudson, J. A. [2000] Fault properties from seismic Q. *Geophysical Journal International*, **143**, 937–944.